

University of Groningen

## Exploring new molecular imaging concepts of prostate cancer

Wondergem, Maurits

**IMPORTANT NOTE: You are advised to consult the publisher's version (publisher's PDF) if you wish to cite from it. Please check the document version below.**

*Document Version*

Publisher's PDF, also known as Version of record

*Publication date:*

2017

[Link to publication in University of Groningen/UMCG research database](#)

*Citation for published version (APA):*

Wondergem, M. (2017). *Exploring new molecular imaging concepts of prostate cancer*. University of Groningen.

### Copyright

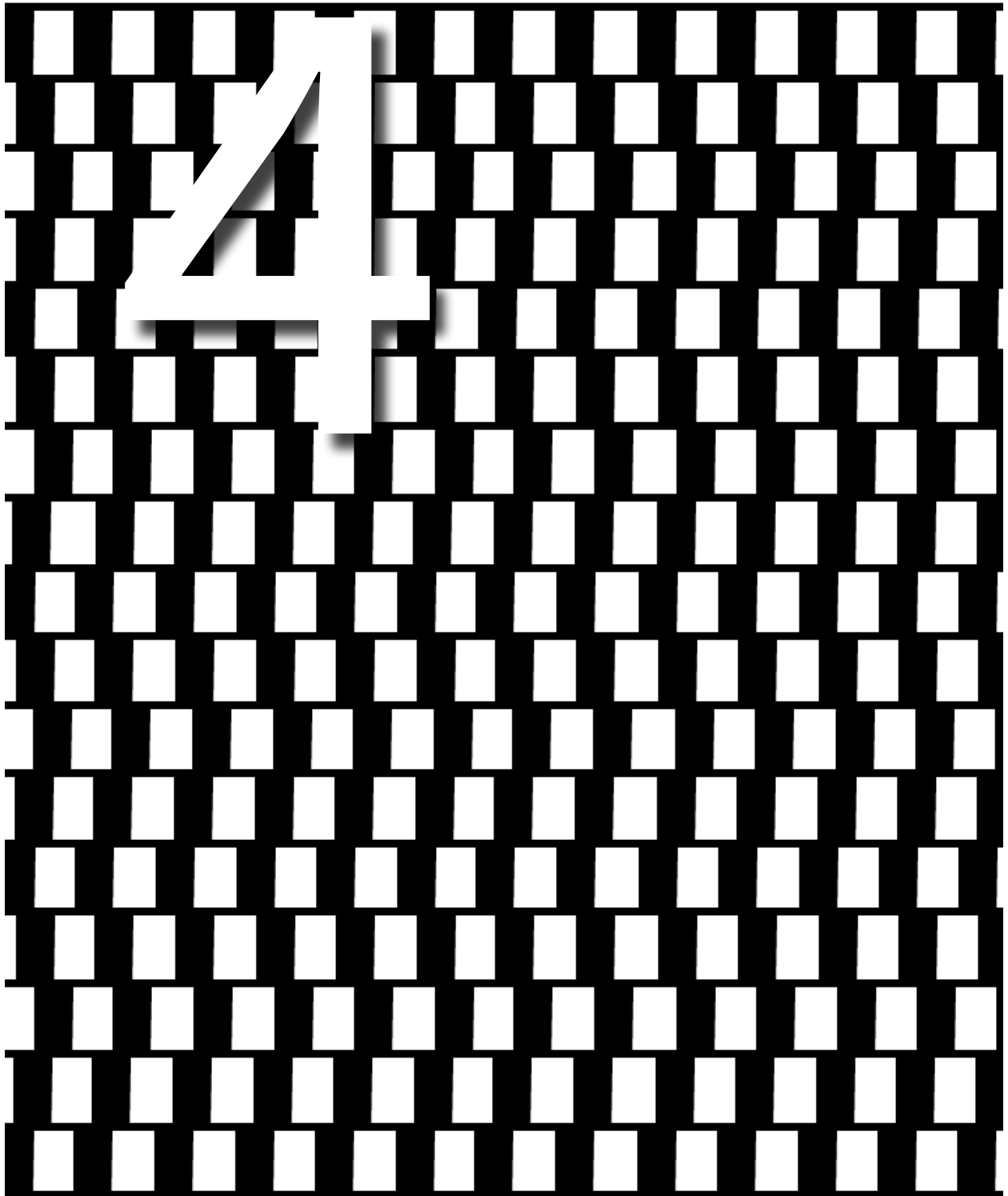
Other than for strictly personal use, it is not permitted to download or to forward/distribute the text or part of it without the consent of the author(s) and/or copyright holder(s), unless the work is under an open content license (like Creative Commons).

The publication may also be distributed here under the terms of Article 25fa of the Dutch Copyright Act, indicated by the "Taverne" license. More information can be found on the University of Groningen website: <https://www.rug.nl/library/open-access/self-archiving-pure/taverne-amendment>.

### Take-down policy

If you believe that this document breaches copyright please contact us providing details, and we will remove access to the work immediately and investigate your claim.

Downloaded from the University of Groningen/UMCG research database (Pure): <http://www.rug.nl/research/portal>. For technical reasons the number of authors shown on this cover page is limited to 10 maximum.





# Kinetic study of $^{18}\text{F}$ -fluorocholine uptake to differentiate malignant and physiologic uptake of $^{18}\text{F}$ -fluorocholine in prostate cancer metastases

Maurits Wondergem<sup>a,c</sup>  
Remco J.J. Knol<sup>a</sup>  
Friso M. van der Zant<sup>a</sup>  
Tjeerd van der Ploeg<sup>b</sup>  
Jan Pruijm<sup>d,e</sup>  
Igle J. de Jong<sup>c</sup>

<sup>a</sup> Department of Nuclear Medicine, Noordwest Ziekenhuisgroep, Alkmaar, The Netherlands

<sup>b</sup> Foreest Medical School, Noordwest Ziekenhuisgroep, Alkmaar, The Netherlands

<sup>c</sup> Department of Urology, University Medical Center Groningen, University of Groningen, Groningen, The Netherlands

<sup>d</sup> Department of Nuclear Medicine and Molecular Imaging, University Medical Center Groningen, University of Groningen, Groningen, The Netherlands

<sup>e</sup> Department of Nuclear Medicine, Tygerberg Hospital, Stellenbosch University, Stellenbosch, South Africa

## ABSTRACT

### Introduction

<sup>18</sup>F-fluorocholine-PET/CT is widely used in patients with prostate cancer. Knowledge of the kinetic behaviour of <sup>18</sup>F-fluorocholine in malignant lesions and normal tissue is helpful in distinguishing malignant from normal <sup>18</sup>F-fluorocholine uptake and to identify a suitable time point after <sup>18</sup>F-fluorocholine administration for acquisition of PET/CT images. We studied characteristics of <sup>18</sup>F-fluorocholine uptake in tissues of importance to detect lymph node and bone metastases. We hypothesized that the most favourable time-point for data acquisition of <sup>18</sup>F-fluorocholine PET/CT in prostate cancer patients is the time-point at which the activity of <sup>18</sup>F-fluorocholine in all tissues that are of importance to detect lymph node and bone metastases is near stable.

### Methods

One hundred subsequent patients with histopathologically proven prostate cancer were prospectively included in the study. Dynamic PET/CT images of the pelvic area were acquired in the first 10 minutes followed by total body images at 45-60 minutes post injection. SUV measurements on different time-points were done in lymph node metastases, non-malignant lymph nodes, bone metastases, normal bone marrow, blood pool, adipose tissue, intestine, and muscle.

### Results

Dynamic data shows a nearly stable <sup>18</sup>F-fluorocholine activity in all tissues from 2 minutes post injection. However significant changes in <sup>18</sup>F-fluorocholine uptake between early and late time-points are detected. A decrease in uptake in non-malignant lymph nodes and blood pool and an increase in muscle, bone metastases and non-malignant bone occurs over time. This results in a statistically significant decrease between early and late time points of the target-to-non-target ratio (TNT) of both bone metastases versus muscle and malignant lymph nodes versus muscle, whereas an increase in TNT is demonstrated between malignant lymph nodes versus blood pool. ROC-analysis shows that  $SUV_{max,late}$  is the best predictor of malignancy in lymph nodes (cut-off 2.0) and  $SUV_{max,early}$  and  $SUV_{max,late}$  (cut-off 2.5 and 2.9 respectively) are the best predictors of malignancy for bone lesions.

### Conclusion

According to our data, a dual time-point acquisition protocol would be favourable over a single time point acquisition for detection of lymph node metastases. For the studied time points  $SUV_{max,late}$  is the best characteristic to discriminate malignant from non-malignant lymph nodes. Increasing <sup>18</sup>F-fluorocholine uptake over time is highly specific for lymph node metastases, while a decrease in <sup>18</sup>F-choline uptake can be seen in both malignant as non-malignant lymph nodes. For detection of bone metastases, an early data acquisition is preferable due to accumulation of activity in muscle at later time points. Both  $SUV_{max,early}$  and  $SUV_{max,late}$  can be used to discriminate malignant bone lesions from non-malignant bone.

## INTRODUCTION

$^{18}\text{F}$ -fluorocholine-PET/CT is widely used in patients with prostate cancer. Clinically, the imaging technique is used mainly for restaging of patients with a biochemical relapse and less frequently for initial staging. One of the strengths of  $^{18}\text{F}$ -fluorocholine-PET/CT is the detection and localisation of prostate cancer metastases in patients with slightly elevated prostate specific antigen blood levels. In early stages prostate cancer metastasises most frequently to regional lymph nodes and bone marrow.

Variability in the reported sensitivity and specificity of  $^{18}\text{F}$ -fluorocholine can be found in literature, probably due to a lack of standardisation of acquisition protocols (1). Studies with relatively small patient populations show different  $^{18}\text{F}$ -fluorocholine time-activity patterns for both non-malignant and malignant lesions. For malignant lymph nodes, patterns that show no difference in  $^{18}\text{F}$ -fluorocholine uptake between early and late measurements, patterns that show a marginal decrease over time and patterns showing increased  $^{18}\text{F}$ -fluorocholine uptake over time, are reported (2-5). For malignant bone lesions reported time-activity patterns differ from a steady state of tracer uptake from approximately 6 min post administration of  $^{18}\text{F}$ -fluorocholine to increasing  $^{18}\text{F}$ -fluorocholine uptake between early and late measurements (2, 6). Based on these different patterns different recommendations are given regarding the time point of image acquisition, including single, dual and triple time point protocols (2, 4, 6). Furthermore,  $^{18}\text{F}$ -fluorocholine uptake is not tumour specific and false positive lymph nodes have been described in literature (1). For those reasons knowledge of the kinetic behaviour of  $^{18}\text{F}$ -fluorocholine in malignant lesions and non-malignant tissues is important to distinguish malignant from non-malignant  $^{18}\text{F}$ -fluorocholine uptake and, in addition, may help to identify the best time point after  $^{18}\text{F}$ -fluorocholine administration for acquisition of PET/CT images.

In this paper we report a kinetic study on  $^{18}\text{F}$ -fluorocholine uptake in both non-malignant tissues and malignant lesions which are thought to be relevant for detection of lymph node and bone marrow metastases in prostate cancer patients. We hypothesized that the most favourable time-point for data acquisition of  $^{18}\text{F}$ -fluorocholine PET/CT in prostate cancer patients is the time-point at which the activity of  $^{18}\text{F}$ -fluorocholine in all tissues that are of importance to detect lymph node and bone metastases is near stable. In a prospective study dynamic data was used to determine the time-point, by means of time-activity curves (TAC), at which the activity of  $^{18}\text{F}$ -fluorocholine in tissues of importance is near stable. Since reports in literature argument that late data acquisition has added value we included a late data acquisition in the study protocol to check for changes between data acquired at the time-point that  $^{18}\text{F}$ -fluorocholine activity was near stable and later data acquisition.

A certain tumour to background ratio is needed for detection of metastases, therefore it is assumed that for detection of metastases on PET scans, knowledge of the time-activity pattern in both metastases and tissues directly adjacent to lymph nodes and

bone is relevant. From our experience we identified tissues that may interfere with detection of metastases. Figure 1 illustrates possible interference of activity in the blood pool, muscle and intestine with detection of lymph node metastases. Lymph nodes are usually surrounded by adipose tissue, therefore the activity uptake in adipose tissue was also assumed relevant for detection of lymph node metastases. In the present study, data was therefore obtained for lymph node metastases and non-malignant lymph nodes, and also for blood pool, muscle, intestine and adipose tissue. Figure 2 illustrates high  $^{18}\text{F}$ -fluorocholine uptake in non-malignant bone marrow and in muscle, which may interfere with bone metastasis detection. For the evaluation of detection of bone metastases, time-activity curves were obtained from the bone metastases, as well as non-malignant bone marrow and muscle.

We aim to provide characteristics that are helpful to distinguish non-malignant from malignant lesions and to provide information whether early, late or both early and late  $^{18}\text{F}$ -fluorocholine PET/CT image acquisition is favourable for patients with prostate cancer.

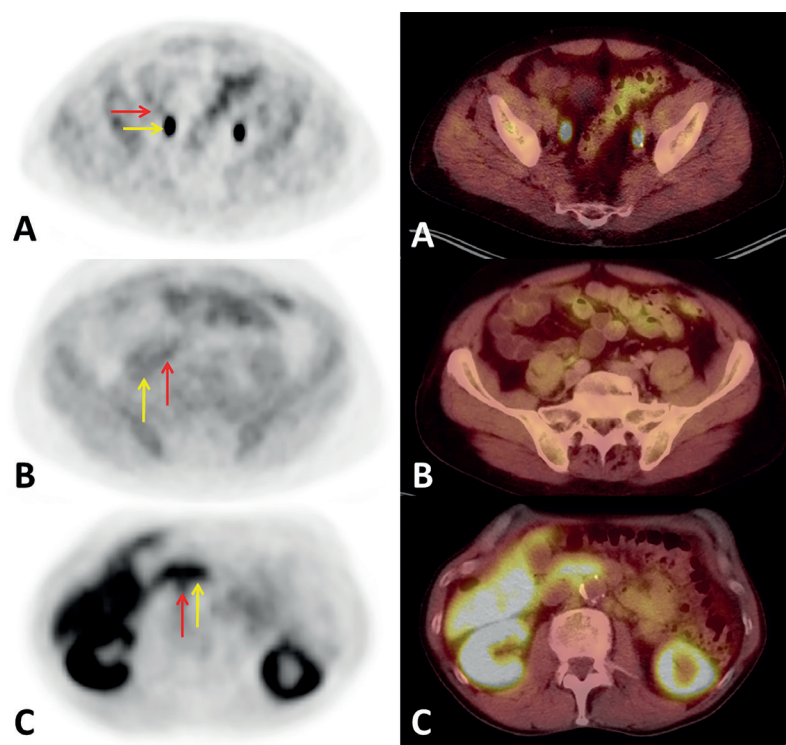


**Figure 1.** Interference of normal  $^{18}\text{F}$ -fluorocholine activity with detection of lymph node metastases. (A) Activity in the blood pool (yellow arrow) interferes with activity in a malignant lymph node (red arrow). (B) Interference of normal muscle activity (yellow arrow) with activity in a malignant lymph node (red arrow). (C) Interference of intestinal activity (yellow arrow) with activity in a malignant lymph node (red arrow).

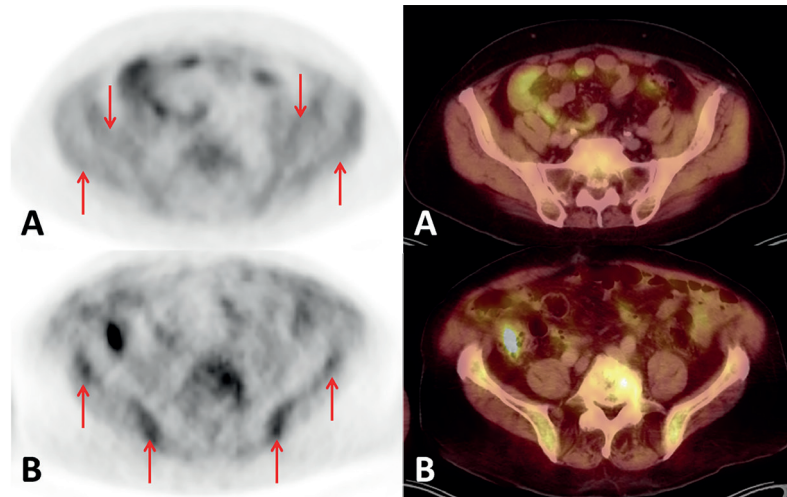


**Figure 2.** Possible interference of normal  $^{18}\text{F}$ -fluorocholine activity with detection of bone metastases. (A) Normal muscle activity (red arrows) and (B) normal bone activity (red arrows) that may interfere with detection of bone metastasis.

4

## MATERIAL AND METHODS

### Patients

From 15 May 2013 until 30 April 2015  $^{18}\text{F}$ -fluorocholine PET/CT scans for staging or restaging of prostate cancer of 100 subsequent referred patients with histopathologically proven prostate cancer were prospectively included in the study. In case of a biochemical relapse  $^{18}\text{F}$ -fluorocholine PET/CT was indicated if PSA > 5 ng/ml, or PSA > 1 ng/ml and a PSA doubling time < 3 months or Gleason score  $\geq 8$  following the Dutch guidelines for prostate cancer (7). Thereby a biochemical relapse was defined by two consecutive PSA values of 0.2 ng/ml and rising after radical prostatectomy and by any PSA increase  $\geq 2$  ng/ml higher than the PSA nadir value, regardless of the serum concentration of the nadir after external radiation therapy or brachytherapy (8). For primary staging purposes  $^{18}\text{F}$ -fluorocholine PET/CT was only used in case of equivocal findings on conventional imaging ( $^{99\text{m}}\text{Tc}$ -HDP,  $^{18}\text{F}$ -sodiumfluoride PET/CT or MRI).

Follow up scans of already included patients and scans of patients known with other malignancies were excluded. Patients characteristics including Gleason score and TNM-classification at time of diagnosis, age, PSA, and PSA doubling time at time of the scan, as well as the date and type of previous therapy were entered in a database. All patients gave written informed consent for the use of their anonymous data for scientific purposes. Approval of the local ethical committee for the present study was not necessary since the study does not fall within the scope of the Medical Research Involving Human Subjects Act (section 16.2 WMO, 26<sup>th</sup> February 1998).



## **Imaging**

Patients were instructed to drink one litre of water in the hour before  $^{18}\text{F}$ -fluorocholine injection. In attempt to avoid high bladder activity concentrations in the bladder at the early time point, patients were encouraged not to void until completion of the early scan sequence. Scans were acquired at an early and a late time point.

$^{18}\text{F}$ -fluorocholine was produced and synthesised by an on-site cyclotron facility according to the Bis(tosyloxy)methane method (Trasis Pharmacy Instruments). Directly after injection of 182 MBq  $^{18}\text{F}$ -fluorocholine (mean; range 126-216 MBq, depending on body weight) list mode (event-by-event) data from the pelvic area were acquired during 10 minutes (early dynamic) on a Siemens Biograph-16 TruePoint PET/CT (Siemens Healthcare, Knoxville, U.S.).

From the list mode data, 10 x 1 min frames were reconstructed by means of a TrueX algorithm using 4 iterations and 8 subsets and a 5 mm Gaussian filter. Reconstructed images had an image matrix size of 168 x 168, a voxel size of 4.07 x 4.07 mm and a slice thickness of 3 mm (early dynamic).

In order to detect differences in  $^{18}\text{F}$ -fluorocholine uptake between the late phase and the early phase, the data obtained between the 4<sup>th</sup>-7<sup>th</sup> minute (early static) from the list mode acquisition were reconstructed with the same parameters that were used to reconstruct the late phase data (late static). The late scan was acquired at 45-60 minutes after injection, with 4 min/bed position, from the proximal femurs to the base of the skull. Reconstruction was done by means of an iterative 3D algorithm using 4 iterations and 8 subsets and a 5 mm Gaussian filter. Reconstructed images had an image matrix size of 168 x 168, a voxel size of 4.07 x 4.07 mm and a slice thickness of 5 mm.

For attenuation correction of the early scan, a low-dose CT was acquired using a tube current of 25 mAs at 130 kV, collimation 16 x 1.2 mm and a pitch of 0.95. A CT with intravenous contrast administration using a tube current of 110 mAs at 110-130 kV, collimation 16 x 1.2 mm and pitch 0.95 was used for attenuation correction of the late images. Both CTs were reconstructed using a matrix size of 512 x 512 resulting in voxel sizes of 1.37 x 1.37 mm and a slice thickness of 5 mm.

## **Lesion selection**

All PET/CTs were read by two experienced Nuclear Medicine Physicians (M.W. and F.Z.). Lymph nodes with elevated tracer uptake compared to normal lymph nodes on the late images were considered malignant. Thereby normal lymph node uptake was defined as uptake not higher than uptake in surrounding adipose tissue. Bone lesions with elevated tracer uptake compared to adjacent bone marrow and without signs of degenerative disease on CT were considered malignant.

Non-malignant tracer uptake in lymph nodes was defined as the uptake measured in the largest lymph node (of at least 4 mm in short axis on CT) in both left and right inguinal

regions and, when present, the largest lymph node in both the left and right iliac regions, excluding those with increased activity on late images. Non-malignant bone activity was defined as the mean uptake in a standard region in the petrochanteric region of the left femur. Blood pool activity was measured in the left external iliac artery; activity in adipose tissue in a standard region on the right lateral side of the bladder; muscle activity in the left gluteal muscle; and intestinal activity was measured as the highest activity  $\leq 1$ cm in the vicinity of the iliac vessels, since interference with detection of malignant lymph nodes in these regions may occur. Only lesions in the field of view of the early data acquisition were included in the analysis. Comparison between early and late static data was only done for patients with suspected malignant lymph nodes and/or bone lesions.

A reference standard (RS) consisting of a follow-up period of at least 9 months was used, during which histopathology reports, imaging (BS,  $^{18}\text{F}$ -sodiumfluoride PET/CT, MRI, CT, X-ray,  $^{18}\text{F}$ -fluorocholine-PET/CT, and/or  $^{18}\text{F}$ -FDG-PET/CT), biochemical follow-up, and clinical follow-up were used to determine whether target lesions were malignant or benign.

4

#### **Data extraction**

From the early dynamic data, kinetic data of  $^{18}\text{F}$ -fluorocholine uptake was extracted by measuring the  $\text{SUV}_{\text{max}}$  at one minute intervals after injection of the tracer in all selected lesions and tissues of interest by means of volume of interest (VOI) analysis (VOI isocontour tool; 40% from maximum) using SyngoVia software (Siemens syngo.via, Siemens Healthcare, Knoxville, USA). This software package was also used to measure the  $\text{SUV}_{\text{max}}$  in each VOI on the early static and late static images. The automatic registration function of the software package was used to align the scans. VOIs from the early dynamic images were copied to early static and late static images. Then, target-to-non target ratio's (TNT-ratio) were calculated based on the  $\text{SUV}_{\text{max}}$  in malignant lymph nodes versus the  $\text{SUV}_{\text{max}}$  in adipose tissue, intestine, muscle, and blood pool. These ratios were also calculated for malignant bone lesions versus normal bone and muscle.

#### **Statistical analysis**

Using the early dynamic data, time activity curves were constructed of all  $\text{SUV}_{\text{max}}$  measurements at an interval of one minute until 10 minutes after injection of  $^{18}\text{F}$ -fluorocholine. The Kolmogorov-Smirnov test was used to check for normal distribution of the data. Since not all data sets showed normality the ANOVA-test and if applicable a post-hoc analysis according to Scheffe's test was used to find significant differences in  $\text{SUV}_{\text{max}}$  between VOIs at a certain time point, using the early dynamic, early static and late static data. According to presence or absence of normality the paired T-test or the Wilcoxon signed rank test was used to test for statistically significant differences between early and late  $\text{SUV}_{\text{max}}$  and early and late TNT-ratios.

In order to find the best predictors for both lymph node and bone status ROC analyses for the characteristics  $SUV_{max,early}$ ,  $SUV_{max,late}$ ,  $SUV_{max,late-early}$ ,  $SUV_{max,(late-early)/early}$ , and velocity of  $^{18}F$ -fluorocholine uptake in the first 2 minutes after injection ( $SUV_{velocity} = (SUV_{min2} - SUV_{min0})/2$ ) with units ( $min^{-1}$ ) were performed.

## RESULTS

A total of 100 consecutive scans were initially included in this study. Four scans were excluded because they proved to be follow-up scans of already included patients and of these, only the first scan was used. Three other scans were excluded for incomplete data storage. None of the included patients had a known second malignancy. As a result, the kinetic data of  $^{18}F$ -fluorocholine of 93 patients was studied (Table 1).

### Lymph nodes

Uptake in non-malignant lymph nodes was measured in a total of 168 lymph nodes of 72 patients. Twenty-three patients showed no lymph nodes >4 mm in both the inguinal and iliac regions. In 35 patients 46 suspected lymph node metastases were detected in the pelvic area. Normal tracer accumulation was measured in 92, 79, 93, and 91 patients in the blood pool, intestine, muscle and adipose tissue, respectively. In one patient no blood pool activity was measured since the tracer was administered at a deviant injection site (vein on dorsal foot instead of antecubital fossa). In 14 patients no activity was present in the intestine within 1 cm of the iliac vessels. Due to a lack of abdominal fat, tracer accumulation in pelvic adipose tissue could not be determined using the standard VOI in 2 patients. According to the RS, presence of malignancy was uncertain in six lymph nodes that were classified as suspicious of malignancy on PET/CT. All other suspicious lymph nodes proved to be malignant according to the RS. No assumed normal lymph nodes were found to be malignant, according to the RS.

### Early dynamic data

The early  $^{18}F$ -fluorocholine time-activity curves of malignant lymph nodes, non-malignant lymph nodes, blood pool, muscle, intestine and adipose tissue are shown in Figure 3. There is a rapid decline in blood pool activity within the first four minutes, after which the activity remains more or less stable. The uptake of  $^{18}F$ -fluorocholine in suspected malignant lymph nodes, non-malignant lymph nodes, muscle, intestine and adipose tissue increases rapidly in the first two minutes, after which a nearly stable tracer accumulation is measured until the tenth minute. At all time-points there is a significantly higher activity in malignant lymph nodes compared to normal lymph nodes, adipose tissue and muscle tissue ( $p < 0.000$  in all instances). Intestine activity in the vicinity of the iliac vessels was seen in 85% of the patients. No significant difference was found between activity in malignant lymph nodes and the intestines.

**Table 1.** Patients characteristics.

No. of patients		93	
Indication <sup>18</sup> F-fluorocholine PET/CT			
	Primary staging	14	
	Biochemical relapse	77	
	Other	2	
Age (years)		70†	51-83‡
PSA at scan (ng/ml)		11,5†	0,24-115,8‡
PSA doubling time (months)		6,1†	1-24‡
Gleason score			
	6	17	
	7	21	
	8	11	
	9	18	
	Unknown	26	
cT-stage at diagnosis			
	1	3	
	2	21	
	3	36	
	4	3	
	Unknown	30	
cN-stage at diagnosis			
	x	17	
	0	34	
	1	10	
	Unknown	31	
Previous therapy			
	None	14	
	Prostatectomy	17	
	External radiation therapy	40	
	Brachytherapy	8	
	HIFU*	3	
	Unknown	11	
Previous salvage therapy			
	None	64	
	External radiotherapy	17	
Patients on hormone therapy at scan			
	Yes	16	
	No	77	

\*High-Intensity Focused Ultrasound, †mean, ‡range

4

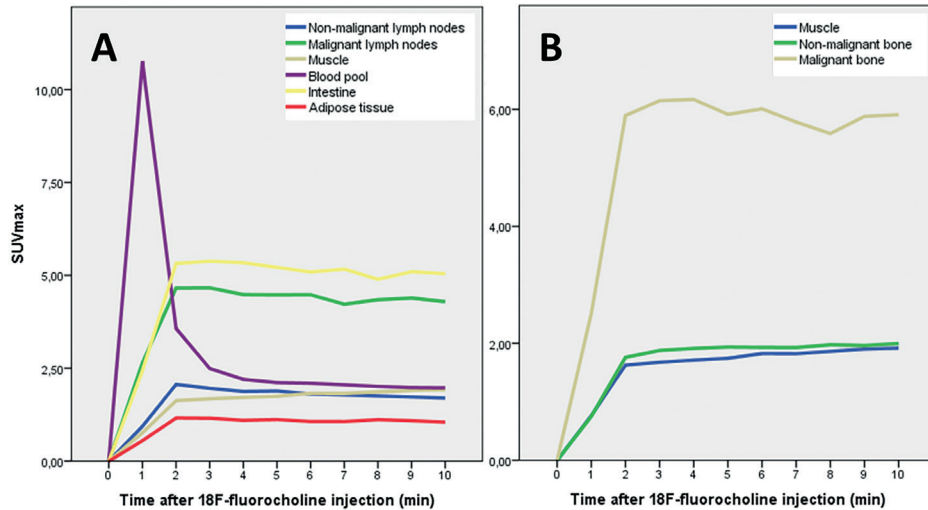


**Figure 3.** Time activity pattern of  $^{18}\text{F}$ -fluorocholine in (A) malignant lymph nodes and adjacent physiologic tissues and (B) malignant bone lesions and adjacent physiologic tissues in the first 10 minutes after intravenous administration. SUVs obtained from dynamic frames cannot be compared with the SUVs obtained from static images.

#### *Early static and late static data*

On the static images, a significant higher  $^{18}\text{F}$ -fluorocholine uptake was measured in malignant lymph nodes compared to normal lymph nodes, adipose tissue and muscle tissue ( $p < 0.000$  in all instances at both time points). No differences were found between the activity in malignant lymph nodes and intestines ( $p = 0.875$  at the early time point and  $0.999$  at the late time point). There was a marginal, but not significant increase of  $^{18}\text{F}$ -fluorocholine uptake in malignant lymph nodes at the late versus the early time point (Table 2). Tracer uptake in normal lymph nodes decreased significantly, as did the blood pool activity, while activity in muscle increased over time ( $p < 0.000$  in all instances). Intestinal and adipose tissue activity was stable over time. The TNT- ratio between malignant lymph nodes versus intestines and adipose tissue was stable over time. A significant increase of the TNT-ratio between malignant nodes and blood pool activity was detected as well as a significant decrease of the TNT-ratio between malignant nodes and muscle activity (both  $p < 0.000$ ; Figure 4).

#### *ROC analysis*

Since the true nature of six suspected lymph nodes could not be established by the RS, two ROC analyses were performed with the assumption that these nodes were either malignant or benign (Figure 5). The analysis showed that, according to our data, the  $\text{SUV}_{\text{max,late}}$  value is the best predictor of malignancy at a cut-off value of 1.9 (nodes assumed malignant) resulting in a sensitivity and specificity of both 97% and at a cut-off value of 2.0 (nodes assumed normal) resulting in a sensitivity of 100% and specificity of 96%. Increasing the SUV cut-off value decreases sensitivity, whereas decreasing the cut-off decreases the specificity.

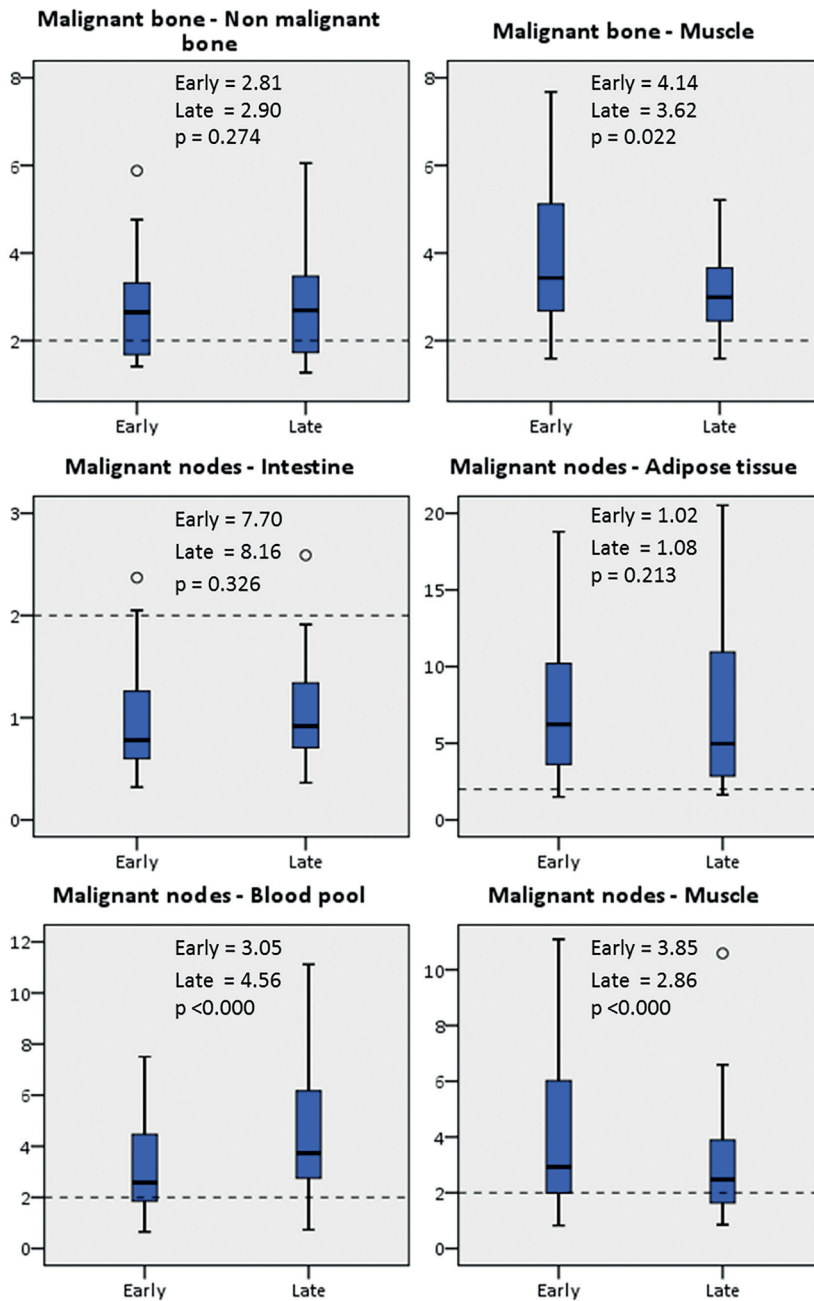


**Figure 4.** Target to non-target ratios between malignant bone lesions and malignant lymph nodes and tissues in their direct proximity. Boxplots and mean SUV values are given for both time-points (Early and Late). Dotted line shows TNT-ratio = 2. All p-values were calculated using a Wilcoxon signed rank test.

**Table 2.** Comparison of early and late <sup>18</sup>F-fluorocholine uptake in different tissues.

		Mean	Std. Deviation	Significance
Malignant lymph nodes	SUV <sub>early</sub>	4.22	2.02	0.158 <sup>‡</sup>
	SUV <sub>late</sub>	4.44	2.54	
Non-malignant lymph nodes	SUV <sub>early</sub>	1.65	0.54	<0.000 <sup>‡</sup>
	SUV <sub>late</sub>	1.16	0.34	
Blood pool	SUV <sub>early</sub>	1.30	0.27	<0.000 <sup>‡</sup>
	SUV <sub>late</sub>	0.96	0.33	
Muscle	SUV <sub>early</sub>	1.35	0.48	<0.000 <sup>‡</sup>
	SUV <sub>late</sub>	1.81	0.55	
Intestine	SUV <sub>early</sub>	4.06 <sup>*</sup>	3.01 <sup>†</sup>	0.787 <sup>§</sup>
	SUV <sub>late</sub>	4.02 <sup>*</sup>	3.83 <sup>†</sup>	
Adipose tissue	SUV <sub>early</sub>	0.69	0.25	0.199 <sup>‡</sup>
	SUV <sub>late</sub>	0.74	0.31	
Malignant bone lesions	SUV <sub>early</sub>	4.68 <sup>*</sup>	2.34 <sup>†</sup>	0.005 <sup>§</sup>
	SUV <sub>late</sub>	5.03 <sup>*</sup>	3.64 <sup>†</sup>	
Non-malignant bone	SUV <sub>early</sub>	1.27 <sup>*</sup>	0.66 <sup>†</sup>	0.003 <sup>§</sup>
	SUV <sub>late</sub>	1.48 <sup>*</sup>	0.87 <sup>†</sup>	

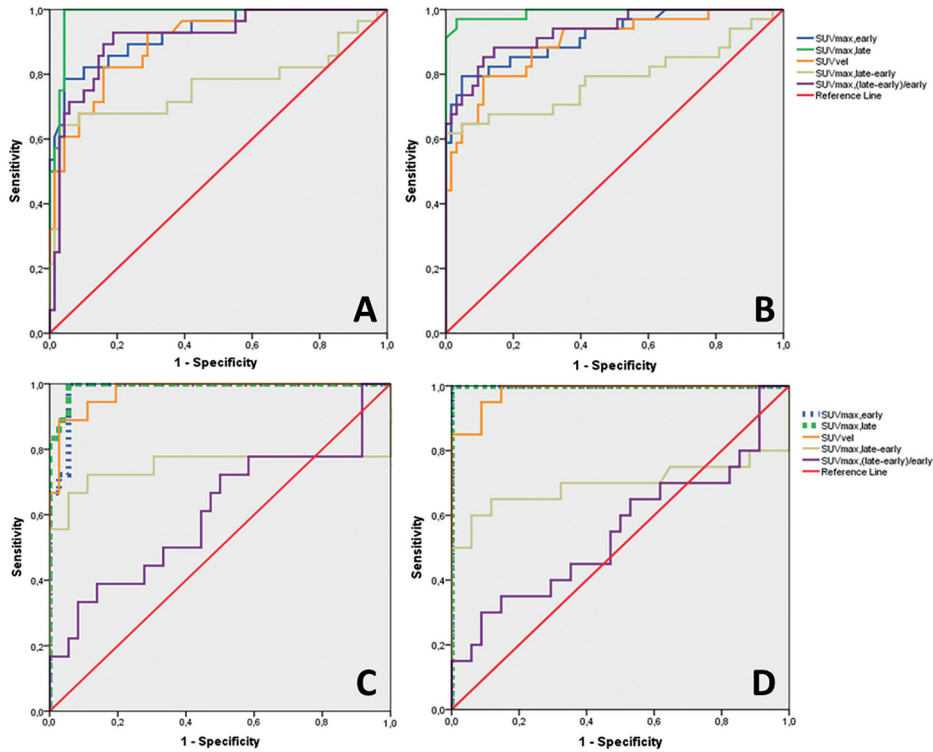
For data not normally distributed: \*Median, †Interquartile range. ‡Paired T-test, §Wilcoxon signed rank test.

### Bone lesions

Non-malignant bone marrow uptake was measured in 90 patients in the left pertrochanteric region. Three patients had a total hip prosthesis and were excluded from evaluation. Muscle activity was measured in all scans. In 11 patients 22 suspected malignant bone lesions were found in the pelvic area. According to the RS, 20 of the suspected bone lesions were malignant, while malignancy in two lesions remained uncertain. No assumed benign bone lesions proved to be malignant.

#### Early dynamic data

Figure 3 shows the time-activity curves from the first 10 minutes after injection of <sup>18</sup>F-fluorocholine in suspected malignant bone lesions, non-malignant bone marrow and muscle. These curves show a rapid increase in the first 2 minutes, followed by a stable phase. In suspected malignant bone lesions the activity is significantly higher compared to normal bone and muscle at all time points (p<0.000 for both).



4

**Figure 5.** ROC-curves for  $SUV_{max,early}$ ,  $SUV_{max,late}$ ,  $SUV_{vel}$ ,  $SUV_{max,late-early}$ ,  $SUV_{max,(late-early)/early}$ . (A) Six unclear lymph nodes assumed non-malignant, (B) all suspected lymph nodes assumed malignant, (C) two unclear bone lesions assumed non-malignant and (D) all suspected bone lesions assumed malignant.

#### Early static and late static data

In accordance with the early dynamic data the  $^{18}F$ -fluorocholine uptake in malignant bone lesions is significantly higher than in normal bone and muscle ( $p < 0.000$  for all) at both time points. Malignant bone lesions ( $p = 0.005$ ), normal bone ( $p = 0.003$ ) and muscle tissue ( $p < 0.000$ ) all show a significant increase of tracer uptake over time (Table 2). As a result, TNT-ratios between malignant bone lesions and normal bone are similar at both time points. The TNT-ratio between malignant bone lesions and muscle, however, decreases significantly over time ( $p = 0.022$ ; Figure 4).

#### ROC analysis

Two ROC analyses were performed with either the assumption that all suspected bone lesions were malignant or that the two lesions, without confirmation according to the RS, were benign (Figure 5). For our data the  $SUV_{max,early}$  and  $SUV_{max,late}$  were found to be the best predictors of malignancy with a cut-off value of 2.5 and 2.9 respectively, irrespective of the chosen assumption. The sensitivity and specificity are both 100% if the two



uncertain lesions are assumed malignant. The sensitivity is 100% and the specificity 94% for both cut-off values if the two uncertain lesions are considered benign. Increasing the SUV cut-off value decreases sensitivity, whereas decreasing the cut-off decreases the specificity.

## DISCUSSION

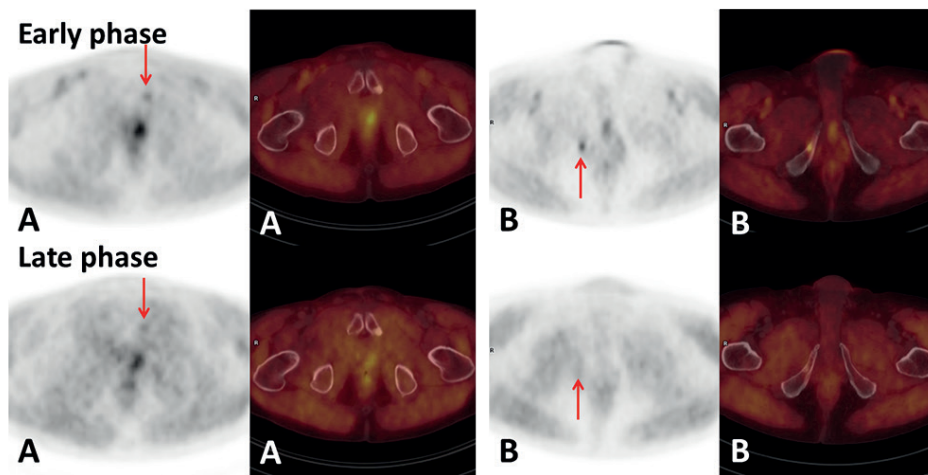
Our data shows that  $^{18}\text{F}$ -fluorocholine uptake in non-malignant and malignant lesions is a rapid process resulting in nearly constant concentrations 2 minutes after injection. However, small but statistically significant changes occur at later time points (45-60 minutes). For clinical practice it is important whether these changes affect the detectability of malignant lesions and the ability to discriminate malignant from benign lesions.

Regarding the detectability of metastases the TNT-ratios between malignant lesions and tissues in their direct surroundings are of importance. In daily clinical practice, detection of metastases depends, at least in part, on the visually notable contrast between lesions with their direct surroundings. As can be seen from Figure 1 normal activity in blood pool, muscle and intestine can hamper detection of lymph node metastases and activity in muscle may likewise interfere with detection of bone metastases (Figure 2). To our knowledge there is no exact cut-off value for the target to non-target ratio for visual detection of malignant lesions in literature. When a cut-off value of 2 is assumed the discrimination between suspected malignant lymph nodes and blood pool activity tends to improve over time, while the ability to discriminate malignant lymph nodes from muscle activity decreases. In general, due to high TNT-ratios,  $^{18}\text{F}$ -fluorocholine has high discriminatory ability between malignant lymph nodes and adipose tissue. In contrast, the TNT-ratios between malignant lymph nodes and intestinal tracer accumulation are generally below 2 at both time points.

For detection of bone metastases the ability to discriminate malignant lesions from activity in muscle is better at the early time point, due to a more progressive  $^{18}\text{F}$ -fluorocholine uptake in muscle tissue than in malignant bone lesions over time. Two examples of better detectability of bone lesions at the early time point are demonstrated in Figure 6. Although no difference between the early and late TNT-ratio was found for the ratio between malignant and non-malignant bone in the group as whole, for single lesions this phenomenon could also be explained by imaging of blood flow in the tumour at the early time point without tracer deposition resulting in absent activity at the late time point (Figure 6 B).

Regarding the ability to discriminate malignant from non-malignant lesions, the ROC-analysis shows that the  $\text{SUV}_{\text{max,late}}$  value discriminates better between malignant and non-malignant lymph nodes than the other characteristics used in the ROC analysis. In addition to this, the uptake pattern of  $^{18}\text{F}$ -fluorocholine in lymph nodes is also helpful in

discriminating normal from malignant lymph nodes. No normal node showed increasing uptake of  $^{18}\text{F}$ -fluorocholine over time. In our analysis, a cut-off value for  $\text{SUV}_{\text{max,late-early}}$  of 0.0 is highly specific (100%) for malignancy, with a modest sensitivity of 62%. Decreasing the cut-off value decreases the specificity. The ROC-analysis for bone lesions shows area under the curves of 1.0 or slightly less for the characteristics  $\text{SUV}_{\text{max,early}}$ ,  $\text{SUV}_{\text{max,late}}$  and  $\text{SUV}_{\text{velocity}}$ . Since we only included bone lesions in the pelvic area scanned on both early and late images, a relatively low number of 22 malignant bone lesions were included in the study, which probably results in these large areas under the curve. However it is not suspected that lesions from other skeletal regions show other  $^{18}\text{F}$ -fluorocholine uptake patterns.



4

**Figure 6.** Two different cases in which a bone metastasis is better seen on early  $^{18}\text{F}$ -fluorocholine PET/CT images. (A) Bone metastasis in inferior ramus of the left pubic bone and (B) in the inferior ramus of the right pubic bone.

In comparison with literature our results, for the uptake pattern in lymph nodes, are in line with results by Cimitan et al. and Price et al (2, 3). In general we found no significant difference between early and late  $^{18}\text{F}$ -fluorocholine uptake in malignant lymph nodes. However in single lymph nodes we found an increasing uptake pattern in 62% of the malignant lymph nodes, consistent with a pattern reported by Oprea et al. (5), and a decreasing pattern in 38%, in line with a pattern described by Steiner et al (4).

Oprea et al. also found that increasing or stable  $^{18}\text{F}$ -fluorocholine activity is a highly specific finding in malignant lymph nodes, which is in agreement with the present study. They found this pattern in 95% of malignant lymph nodes, while in our cohort this pattern was found in only 62% of the malignant lymph nodes. As a result of this difference they found that  $\text{SUV}_{\text{max,(late-early)/early}}$  was the best predictor of malignancy followed by  $\text{SUV}_{\text{max,late}}$  and  $\text{SUV}_{\text{max,late-early}}$  while in our cohort  $\text{SUV}_{\text{max,late}}$  was the best predictor of malignancy.

Differences in acquisition time points between the studies or the small number of malignant lymph nodes in both studies may explain these differences.

Although, in both the study by Oprea et al. and our cohort, most malignant lymph nodes show increasing uptake patterns, other studies show that there are also malignant lymph nodes that show a decreasing activity over time. In our cohort, even in a single patient, increasing and decreasing uptake patterns in malignant lymph nodes were observed. It may be hypothesised that the presence of reactive changes in lymph nodes with metastases may influence the uptake pattern over time, although evidence from the literature is lacking. Thereby reactive changes may cause a decrease in  $^{18}\text{F}$ -fluorocholine accumulation over time.

In comparison with literature, our finding of progressive uptake of  $^{18}\text{F}$ -fluorocholine over time in malignant bone lesions is in line with the report of Cimitan et al (2), who studied early (<15 min) and late (>60min)  $^{18}\text{F}$ -fluorocholine uptake in 100 patients. DeGrado et al (6) described a stable pattern based on measurements until 20 minutes post injection in only a single malignant lesion. To our knowledge no other studies report  $^{18}\text{F}$ -fluorocholine uptake in bone lesions.

A limitation of our study may be the use of CT with diagnostic properties and intravenous contrast for attenuation correction for the late images, while attenuation correction for early images was done with a low dose CT without intravenous contrast. Literature on the effects of intravenous (IV) contrast enhanced CT on SUV measurements in  $^{18}\text{F}$ -fluorocholine PET/CT is absent. However the used technique is similar to  $^{18}\text{F}$ -FDG PET/CT. Studies on this topic in  $^{18}\text{F}$ -FDG PET/CT have shown that the clinical impact of contrast enhanced CT on SUV measurements is absent or negligible (9-11). The standardization protocol for  $^{18}\text{F}$ -FDG PET/CT by Boellaard et al, however, advises that no contrast agent be used until it has been established that attenuation artefacts are completely absent when used during AC-CT (12). Since the  $^{18}\text{F}$ -fluorocholine PET/CT images were acquired in a standard clinical setting and given the advantages of enhanced CTs with intravenous contrast, especially the characterization of lymph nodes adjacent to vascular structures or ureters, late total body images were acquired in combination with IV-contrast enhanced CT. SUV values in tissue which show contrast enhancement such as the lymph nodes and blood pool may therefore be somewhat higher in the late phase. For normal lymph nodes and the blood pool we found a significant decrease in  $\text{SUV}_{\text{max}}$  over time. If IV contrast affected the SUV measurements the found difference would be even higher in reality. For malignant lymph nodes we found no significant difference between early and late SUV and it cannot be ruled out completely that the usage of IV contrast has had no effect on these measurements. Those who do not use IV contrast in standard clinical  $^{18}\text{F}$ -fluorocholine PET/CT should therefore interpret some of the results cautiously.

Another limitation of the study is the use of a reference standard, which comprised of a clinical follow up instead of the gold standard, which is generally assumed to be histopathological confirmation of all lesions. However it is practically impossible and ethically inappropriate to get histopathological confirmation of both all malignant and all non-malignant tissues/lesions included in this study. On the other hand, a strong point of the study is the analysis of <sup>18</sup>F-fluorocholine in both malignant lesions, non-malignant lesions and normal metabolism in tissue in the direct proximity of those lesions, while other studies commonly support their recommendations only on uptake patterns of malignant lesions.

Determination of the best time point for image acquisition requires acquisition of data at various time points after injection. Although we provide data on <sup>18</sup>F-fluorocholine activity for each minute during the first 10 minutes after <sup>18</sup>F-fluorocholine injection, for later time points we only provide data for one late time point. Therefore the best time point for image acquisition cannot be extracted from our data, however in our data we found advantages for combined early and late data acquisition compared to a single time point acquisition. The found “best” discriminators between malignant and normal lymph nodes and bone and the accompanying cut-off values as found by ROC-analysis, cannot be extrapolated to everyone’s clinical practice since parameters that influence the found cut-off, such as used PET-camera, administered dose, acquisition protocol and reconstruction parameters may vary amongst nuclear medicine departments.

Malignant and benign uptake in the prostate region was not studied since both sensitivity and specificity of <sup>18</sup>F-fluorocholine uptake for lesions in the prostate are moderate. Furthermore it is generally accepted that for evaluation of the prostatic region early imaging should be performed because of high physiological <sup>18</sup>F-fluorocholine activity in the urinary tract, which is typically present within a few minutes after intravenous injection of <sup>18</sup>F-fluorocholine (13).

There is growing evidence that PET/CT with <sup>68</sup>Ga or <sup>18</sup>F-PSMA ligands are more sensitive and specific than <sup>18</sup>F-fluorocholine PET/CT (14, 15). However the evidence is based on comparison of <sup>68</sup>Ga-PSMA and <sup>18</sup>F-fluorocholine in small cohorts or <sup>68</sup>Ga-PSMA is only performed in patients without positive findings on <sup>18</sup>F-fluorocholine PET/CT and none of the reported studies comparing <sup>18</sup>F-fluorocholine and <sup>68</sup>Ga-PSMA fulfil all essential requirements for reporting of diagnostic accuracy studies according to the Standards for Reporting Diagnostic Accuracy (STARD 2015) (16). Therefore the level of evidence that <sup>68</sup>Ga-PSMA PET/CT is more accurate than <sup>18</sup>F-fluorocholine PET/CT is still low. In addition, the reports in literature show a lack of standardisation of <sup>18</sup>F-fluorocholine PET/CT acquisition protocols. Our data suggests that single time point acquisition protocols may result in lower sensitivities and/or specificities for detection of lymph node metastases for <sup>18</sup>F-fluorocholine PET/CT. Therefore we suggest that, for a fair comparison, clinical studies comparing <sup>18</sup>F-fluorocholine PET/CT with <sup>68</sup>Ga-PSMA PET/CT should use standardized acquisition protocols including early and late image acquisition.

## **CONCLUSION**

In conclusion,  $^{18}\text{F}$ -fluorocholine uptake in non-malignant and malignant lesions is a rapid process resulting in nearly constant concentrations 2 minutes after injection however, statistically significant and clinically important changes occur at later time points after injection (45-60 min).

Therefore, for lymph nodes, acquisition of images at two time points probably yields the highest accuracy. For bone lesions our data shows that early acquisition of images yields the highest detection rate of bone metastases.

## **ACKNOWLEDGEMENTS**

The authors wish to acknowledge Nick Hoogvorst for his assistance in data extraction from the early static and late static  $^{18}\text{F}$ -fluorocholine data. We also wish to acknowledge our Medical Physicists, Walter Kool and Sergiy Lazarenko, for their consultation on medical physical issues.

## REFERENCES

1. Evangelista L, Zattoni F, Guttilla A et al. Choline PET or PET/CT and biochemical relapse of prostate cancer, A systematic review and meta-analysis. *Clin Nucl Med*. 2013; 38: 305-314.
2. Cimitan M, Bortolus R, Morassut S et al. <sup>18</sup>F-fluorocholine PET/CT imaging for the detection of recurrent prostate cancer at PSA relapse: experience in 100 consecutive patients. *Eur J Nucl Med Mol Imaging*. 2006; 33: 1387-1398.
3. Price DT, Coleman RE, Liao RP et al. Comparison of <sup>18</sup>F-fluorocholine and <sup>18</sup>F-fluorodeoxyglucose for positron emission tomography of androgen dependent and androgen independent prostate cancer. *J Urol*. 2002; 168: 273-280.
4. Steiner Ch, Veas H, Zaidi H et al. Three-phase <sup>18</sup>F-fluorocholine PET/CT in the evaluation of prostate cancer recurrence. *Nuklearmedizin*. 2009; 48: 1-9.
5. Oprea-Lager DE, Vincent AD, van Moorselaar RJA et al. Dual-phase PET-CT to differentiate <sup>18</sup>F-fluoromethylcholine uptake in reactive and malignant lymph nodes in patients with prostate cancer. *PLoS One*. 2012; 7:e48430.
6. DeGrado TR, Coleman RE, Wang S et al. Synthesis and evaluation of <sup>18</sup>F-labeled choline as an oncologic tracer for positron emission tomography: initial findings in prostate cancer. *Cancer Res*. 2000; 61: 110-117.
7. National Dutch Guideline Prostate Cancer version 2.1. Dutch Association of Urology. IKNL website. <http://www.oncoline.nl/prostaatcarcinoom>. Updated September 15, 2016. Accessed December 5, 2016.
8. Mottet N, J Bellmunt, E Briers, RCN van den Bergh, M Bolla, NJ van Casteren, et al. Guidelines on Prostate Cancer. European Association of Urology website. <http://www.uroweb.org>. Update March 2015. Accessed September 9, 2016.
9. Verburg FA, Kuhl CK, Pietsch H et al. The influence of different contrast medium concentrations and injection protocols on quantitative and clinical assessment of FDG-PET/CT in lung cancer. *Eur J Radiol*. 2013; 10: 617-622.
10. Aschoff P, Plathow C, Beyer T et al. Multiphase contrast-enhanced CT with highly concentrated contrast agent can be used for PET attenuation correction in integrated PET/CT imaging. *Eur J Nucl Med Mol Imaging*. 2012; 2 :316-325.
11. Malawi O, Erasmus JJ, Munden RF et al. Quantifying the effect of IV contrast media on integrated PET/CT: clinical evaluation. *AJR Am J Roentgenol*. 2006; 186: 308-309.
12. Boellaard. Standards for PET Image Acquisition and Quantitative Data Analysis. *J Nucl Med* 2009; 50:11S-20S.
13. Simone G, Battista Di Pierro G, Papalia R et al. Significant increase in detection of prostate cancer recurrence following radical prostatectomy with an early imaging acquisition protocol with <sup>18</sup>F-fluorocholine positron emission tomography/computed tomography. *World J Urol*. 2015; 33: 1511-1518.



14. Afshar-Oromeih A, Zechmann CM, Malcher A et al. Comparison of PET imaging with  $^{68}\text{Ga}$ -labelled PSMA ligand and  $^{18}\text{F}$ -choline-based PET/CT for diagnosis of recurrent prostate cancer. *Eur J Nucl Med Mol Imaging*. 2014; 41:11-20.
15. Bluemel C, Krebs M, Polat B et al.  $^{68}\text{Ga}$ -PSMA-PET/CT in patients with biochemical prostate cancer recurrence and negative  $^{18}\text{F}$ -choline-PET/CT. *Clin Nucl Med*. 2016, epub ahead of print.
16. Bossuyt PM, Reitsma JB, Bruns DE et al. STARD 2015: an updated list of essential items for reporting diagnostic accuracy studies. *BJM*. 2015; 351:h5527.

4



